

Modeling and Model Predictive Control (MPC) of an Underwater Double Inverted Pendulum (UDIP)

Éverton L. de Oliveira, Gabriel S. Belém, Victor B.R.A. Pereira, Reginaldo Cardoso and Décio C. Donha

*Lab. of Dynamics and Control (LDC), Dept. of Mechanical Engineering, University of São Paulo (USP)
Av. Prof. Mello Moraes, 2231, 05508-030, São Paulo - SP, Brazil*

ev_lins@usp.br, gbelem4@usp.br, victor.benito1@usp.br, reginaldo.cardoso@usp.br, decdonha@usp.br

Abstract. The Inverted Double Pendulum (IDP) is a classical nonlinear and unstable mechanical system used as a benchmark model for the application of innumerable control techniques. However, such a model was never treated in an off-the-self environment, which represents a gap in its applications range since the demand for underwater robotics is increasing together with the ocean engineering activities. Thus, to fill this gap and build a new benchmark model for the control development of underwater robotics, this paper presents the modeling and control of an Underwater Double Inverted Pendulum (UDIP). The dynamic model is formulated using the formalism of Analytical Mechanics and considering the pertinent hydrodynamic and hydrostatic effects. To keep straight with the control techniques trends, a Model Predictive Control (MPC) is designed for the UDIP. This controller is tested through numerical simulations in MATLAB/Simulink© environment considering two scenarios: 1) in the absence of disturbances, and 2) in the presence of a time-varying water current. The obtained results for the disturbances case reveal an increase in the control effort in comparison with the case without disturbances. In such a way, this reflect the difficulty associated to the control of underwater robots in unstructured environments.

Keywords: Underwater Double Inverted Pendulum, Model Predictive Control, Underwater Robotics.

1 Introduction

The Double Inverted Pendulum (DIP) is a nonlinear and unstable mechanical system used as a benchmark model for the application of innumerable control techniques on different problems, such as the stabilization of a rocket's takeoff or its trajectory control (Moss [1]), or even on the stabilization of prostheses (Rusaw and Ramstrand [2]). About the recurrent works, Sultan and Farej [3] developed a Linear Quadratic Regulator (LQR) for a heavy DIP. The simulations results considering the linearized version of the dynamic model showed good transient response. In Moysis [4], the performance of a LQR was compared against a MPC based on Laguerre functions on the stabilization of a DIP. The results show that the MPC is capable of performing the stabilization of the DIP with a better transient response than the LQR for the cart's position. Similarly, Krafes et al. [5] presented a comparison between a Proportional Integral Derivative (PID) controller and a LQR on the stabilization of a DIP. The simulations showed that both controllers can stabilize the DIP when referring to the nominal case. However, when disturbances are added to the systems, only the LQR is able to stabilize the double pendulum. This happens because the PID is not robust to disturbances since its gain margin is negative (Krafes et al. [5]). Moreover, Mohan et al. [6] proposed a Modified Neuro Fuzzy Controller (MNFC) for the stabilization problem of a DIP. The simulations results and a detailed comparative analysis confirm the superior performance of MNFC over a LQR, an adaptive Fuzzy Logic Controller (FLC) and a Genetic algorithm tuned Fuzzy Controller (GFC). However, the algorithm of Mohan et al. [6] has a relatively complex structure, which can difficult its application. Hasnain et al. [7] presented a new perspective over the classical inverted pendulum problem by modeling and control of an Underwater Inverted Pendulum (UIP). Such a model was proposed to evaluate the effects of hydrodynamic forces and test the stabilization of the UIP with a vibrational control technique. The simulation results showed that, depending on the frequency and amplitude of the introduced vibration, the UIP tends to stabilize around its upright position.

Despite the variety of controllers developed for the DIP, this model was never treated in an off-the-self environment. This represents a gap in its applications range since the demand for underwater robotics is increasing with the ocean engineering activities associated to resources exploration and so on. For sake of example, the modeling and control of a UDIP on the underwater environment can generate important insights about the dynamics

of an Underwater Vehicle-Manipulator System (UVMS). Being more precise, the dynamic coupling between the Underwater Unmanned Vehicle (UUV) and a robotic manipulator can be investigated with a simpler mathematical model due to the similarities between the two systems. This can bring new understandings about this phenomenon that on the underwater environment is a disturbance to the UUV, but on-land is used to stabilize the double pendulum. Therefore, to fill this gap and build a new benchmark model for the control design of underwater robotics systems, this paper presents the modeling and control of an Underwater Double Inverted Pendulum (UDIP). The proposed dynamic model is established based on the classical Euler-Lagrange approach of the Analytical Mechanics, considering modified versions of the energy functions to include hydrodynamics and hydrostatic effects. Semi-empirical models already validated on literature are used to model the nonconservative effects associated with the hydrodynamic drag. Also, to keep straight with the trends for control system design and take benefit of the established mathematical model, an adaptive discrete-time MPC controller is developed for the UDIP. Numerical simulations are done to test the controller in different scenarios, like still water or considering the disturbances induced by a time-varying water current.

The remainder of this paper is organized as follows. In Section 2, the detailed model of the UDIP is developed. Section 3 introduces the design of the MPC controller and the numerical simulations are presented in Section 4. Finally, the conclusions are stated in Section 5.

2 Modeling

The UDIP idealized is composed of a horizontal cart and a vertical double pendulum with cylindrical shaped links. The motion of the system is restricted to the vertical plane, as shown in Figure 1. On that, $N = (O, X, Y)$ is the Cartesian coordinated system attached to the inertial reference frame, while $S_i = (O_i, \hat{x}_i, \hat{y}_i)$, with $i = 1, 2, 3$ bodies, and $S_{ee} = (O_{ee}, \hat{x}_{ee}, \hat{y}_{ee})$ are, respectively, the body-fixed and end-effector reference frames. $x(t)$ is the absolute horizontal displacement of the cart (measured between N and S_1), whereas $\theta_2(t)$ and $\theta_3(t)$ are the absolute angular displacements of the double pendulum joints (measured between the vertical direction and the body-fixed axis \hat{x}_2 and \hat{x}_3 , on the clock-wise sense, correspondingly). Still in Figure 1, the points CG_i and CB_i are the Center of Gravity (CoG) and Center of Buoyancy (CoB, which is the point where the buoyance force is applied) associated to the i -th body, respectively. Also, the UDIP is actuated by a horizontal motor force that drives the cart, $f(t)$, and it is subjected to the disturbances induced by a time-varying water current, $U_\infty(t)$, which is assumed to be parallel to the horizontal direction (irrotational).

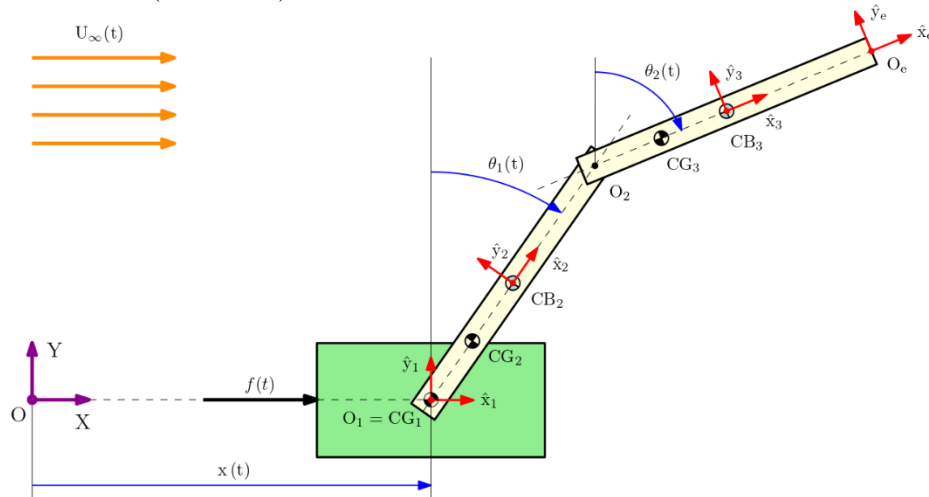


Figure 1. UDIP's schematic diagram

2.1 Equations of motion

Let $\mathbf{q} = [x(t) \ \theta_1(t) \ \theta_2(t)]^T$ be the vector of generalized coordinates of the system. Thus, the equations of motion of the UDIP based on the Euler-Lagrange approach can be written as follows (in matrix form):

$$\frac{d}{dt} \left(\frac{\partial \mathcal{L}}{\partial \dot{\mathbf{q}}} \right) - \frac{\partial \mathcal{L}}{\partial \mathbf{q}} = \mathbf{Q} \Leftrightarrow \mathbf{M}\ddot{\mathbf{q}} + \mathbf{C}\dot{\mathbf{q}} + \mathbf{D} + \mathbf{G} = \mathbf{d} + \boldsymbol{\tau}, \quad (1)$$

where $\mathcal{L} = T - U$ is the Lagrangian function of the systems, with T as the kinetic energy and U as the potential energy functions (on the left side); $\mathbf{Q} = [Q_j]$, with $j = 1, 2, 3$, are the non-conservative generalized forces associated with the j -th generalized coordinate; \mathbf{M} is the generalized inertia matrix, \mathbf{C} is the Coriolis and centrifugal effects matrix, \mathbf{D} is the drag forces vector, \mathbf{G} is the restoring forces vector, \mathbf{d} is the disturbances forces vector, and $\boldsymbol{\tau}$ is the control forces vector (on the right side), which is given by: $\boldsymbol{\tau} = [f(t), 0, 0]^T$.

2.2 Kinetic energy (rigid body and added mass effects)

The kinetic energy of the UDIP, considering the rigid body portion and added mass effects, can be written in terms of the contribution of the i -th body, as follows:

$$\mathcal{T} = \frac{1}{2} \sum_{i=1}^3 (\dot{\mathbf{q}}_i^N)^T \mathbf{M}_i \dot{\mathbf{q}}_i^N, \quad (2)$$

where $\dot{\mathbf{q}}_i^N = [(\mathbf{v}_{CG_i}^N)^T, \omega_{iN}^N]^T$ is the velocity vector, with $\mathbf{v}_{CG_i}^N$ as the absolute velocity vector of the CoG and ω_{iN}^N as the absolute angular velocity; $\mathbf{M}_i = \mathbf{M}_{RB,i} + \mathbf{M}_{A,i}$ is the mass matrix, where $\mathbf{M}_{RB,i}$ is the rigid body mass matrix, and $\mathbf{M}_{A,i}$ is the added mass tensor per say, which is given by: $\mathbf{M}_{A,i} = (\mathbf{R}_i^N)^T \hat{\mathbf{M}}_{A,i} \mathbf{R}_i^N$, where \mathbf{R}_i^N is the rotation matrix from S_i to N and $\hat{\mathbf{M}}_{A,i}$ is local added mass tensor, expressed in the S_i . Indeed, as exposed in Newman [10] and Fossen [11], the added mass tensor has terms dependent on the oscillation frequency. However, it is assumed oscillations at very slows motion, such that the asymptotic limit at zero frequency can be considered for the added mass tensor and this can be taken as constant.

2.3 Potential energy (restoring forces)

The generalized restoring forces of the systems are due to the buoyance and weight forces on each submerged body, also known as hydrostatic forces. These forces can be used to write a generalized potential so that it can be associated to the potential energy function of the UDIP, as follows:

$$\mathcal{U} = \sum_{i=1}^3 (\mathbf{F}_{W_i}^N)^T \mathbf{p}_{CG_iO}^N - (\mathbf{F}_{B_i}^N)^T \mathbf{p}_{CB_iO}^N, \quad (3)$$

being $\mathbf{p}_{CG_iO}^N$ and $\mathbf{p}_{CB_iO}^N$ the absolute position vectors of the CoG and CoB of the, respectively; $\mathbf{F}_{W_i}^N$ and $\mathbf{F}_{B_i}^N$ are the weight and the buoyance force vectors, correspondingly, which are given by:

$$\mathbf{F}_{W_i}^N = [0 \ -m_i g \ 0]^T; \quad \mathbf{F}_{B_i}^N = [0 \ \rho V_i g \ 0]^T, \quad (4)$$

with m_i and V_i as the mass and the displaced volume of the i -th body, respectively; g is the gravity's acceleration on the vertical direction and ρ is the water density.

2.4 Drag forces (hydrodynamic damping)

Concerning the modeling of viscous drag forces, Leabourne and Rock [8] developed a model for the hydrodynamic drag forces of a two-link planar underwater manipulator. This model is similar to the one of McLain and Rock [9] for the hydrodynamic forces on a single-link underwater arm. However, an additional term is included on the model of Leabourne and Rock [8] to consider the drag force developed on the end-effector of the manipulator. Such model is based on the Morison's equation and on the strip theory by means of the discretization of the links into strips. Thus, considering the model of Leabourne and Rock [8], the vector of generalized drag forces for the UDIP is given by:

$$\mathbf{D} = - \sum_{i=1}^3 \sum_{k=1}^{n_s} (\mathbf{F}_{S_k}^i)^T \frac{\partial \mathbf{v}_{S_k}^i}{\partial \dot{\mathbf{q}}} - (\mathbf{F}_{ee}^{ee})^T \frac{\partial \mathbf{v}_{ee}^{ee}}{\partial \dot{\mathbf{q}}}, \quad (5)$$

where $\mathbf{v}_{S_k}^i$ is the absolute velocity vector of the k -th strip expressed in S_i , for $k=0, \dots, n_s$ strips (considering equally discretized bodies), \mathbf{v}_{ee}^{ee} is the absolute velocity vector of the end-effector expressed in S_{ee} ; $\mathbf{F}_{S_k}^i$ is the drag forces vector of the k -th strip and \mathbf{F}_{ee}^{ee} is the drag force on the end-effector, as shown below:

$$\mathbf{F}_{S_k}^i = [f_{S_k, \hat{x}_i} \ f_{S_k, \hat{y}_i} \ 0]^T; \quad \mathbf{F}_{ee}^{ee} = [f_{ee} \ 0 \ 0]^T, \quad (6)$$

with f_{S_k, \hat{x}_i} and f_{S_k, \hat{y}_i} as the drag components of the k -th strip and f_{ee} as the drag force of the end-effector. According to Leabourne and Rock [8], these forces can be calculated through the Morison's equation as a function of the relative velocity between the strip and the water current, as follows:

$$f_{S_k, \hat{x}_i} = \frac{1}{2} \rho C_{D, \hat{x}_i} |\mathbf{v}_{r, S_k, \hat{x}_i}^i| \mathbf{v}_{r, S_k, \hat{x}_i}^i A_{\hat{x}_i}; \quad f_{S_k, \hat{y}_i} = \frac{1}{2} \rho C_{D, \hat{y}_i} |\mathbf{v}_{r, S_k, \hat{y}_i}^i| \mathbf{v}_{r, S_k, \hat{y}_i}^i A_{\hat{y}_i}; \quad f_{ee} = \frac{1}{2} \rho C_{D, ee} |\mathbf{v}_{r, ee, \hat{x}_{ee}}^{ee}| \mathbf{v}_{r, ee, \hat{x}_{ee}}^{ee} A_{ee}, \quad (7)$$

where $\mathbf{v}_{r, S_k, \hat{x}_i}^i$ and $\mathbf{v}_{r, S_k, \hat{y}_i}^i$ are the local components of the relative velocity vector of the k -th strip; $\mathbf{v}_{r, ee, \hat{x}_{ee}}^{ee}$ is the local component on the \hat{x}_{ee} direction of the relative velocity vector of the end-effector; $A_{\hat{x}_i}$, $A_{\hat{y}_i}$ and A_{ee} are the reference areas projected on the local directions, which are given by: $A_{\hat{x}_i} = B_i H_i$, $A_{\hat{y}_i} = 0$, $A_{\hat{x}_i} = \pi D_i \Delta_i$, $A_{\hat{y}_i} = D_i \Delta_i$ (for $i=2,3$) and $A_{ee} = \pi D_3^2 / 4$, where B_i and H_i are the front area dimensions of the cart, D_i and Δ_i are the diameter and strip's length of the i -th link, respectively, while D_3 is the diameter of the end-effector; C_{D, \hat{x}_i} , C_{D, \hat{y}_i} and $C_{D, ee}$ are the drag coefficients on the local directions, which are highly dependent on the flow conditions. Such a dependency can be expressed in terms of the system's configuration and incorporated into the model with experimentally identified coefficients as in Leabourne and Rock [8] or McLain and Rock [9]. However, in this work, it is adopted a conservative approach in the sense of producing an overestimation of the drag forces. For this purpose, the drag coefficients are assumed to be constant.

2.5 Disturbances modeling (time-varying water current)

The relative velocity components are already taken into account in the drag forces. Therefore, only the inertial effects associated with the water current need to be modeled. So, following Fossen [11], these can be expressed as a pair of inertial forces proportional to the augmented mass and Coriolis matrices, as shown below:

$$\mathbf{d} = \mathbf{M}_{\text{FKA}} \dot{\mathbf{v}}_{\infty}^N + \mathbf{C}_{\text{FKA}} \mathbf{v}_{\infty}^N, \quad (8)$$

where $\mathbf{v}_{\infty}^N = [U_{\infty}, 0, 0]^T$ is the current (irrotational) velocity vector, while \mathbf{M}_{FKA} and \mathbf{C}_{FKA} are, respectively, the augmented mass and Coriolis matrices, associated with the added mass tensor and Froud-Krilov terms, as follows:

$$\mathbf{M}_{\text{FKA}} = \sum_{i=1}^3 \mathbf{M}_{\text{FKA},i}; \quad \mathbf{C}_{\text{FKA}} = \sum_{i=1}^3 \mathbf{C}_{\text{FKA},i}, \quad (9)$$

with

$$\mathbf{M}_{\text{FKA},i} = \mathbf{J}_{\text{CG}_i}^i (\hat{\mathbf{M}}_{\text{FK},i} + \hat{\mathbf{M}}_{\text{A},i}) (\mathbf{R}_i^N)^T; \quad \mathbf{C}_{\text{FKA},i} = \mathbf{J}_{\text{CG}_i}^i (\hat{\mathbf{M}}_{\text{FK},i} + \hat{\mathbf{M}}_{\text{A},i}) (\mathbf{R}_i^N)^T (\mathbf{S}_i)^T, \quad (10)$$

being $\mathbf{J}_{\text{CG}_i}^i = [\partial \mathbf{v}_{\text{CG}_i}^i / \partial \dot{\mathbf{q}}]$ the Jacobian matrix of the CoG and \mathbf{S}_i the screw symmetric matrix associated with the rotation \mathbf{R}_i^N , i.e., $\dot{\mathbf{R}}_i^N = \mathbf{S}_i \mathbf{R}_i^N$.

3 Control design

The block diagram of the proposed adaptive discrete-time MPC is shown in Figure 2. The followings steps summarize the whole control process:

- 1) the controller receives a reference, $\mathbf{r}(k)$, at the time instant $t = kT_s$, with $k = 0, 1, 2, \dots, N$ steps and T_s denoting the sampling time;
- 2) based on the dynamic model of the systems and on the current state vector, $\mathbf{x}(k)$, an optimization process is performed over the prediction horizon, p , to minimize a cost function associated to the error between the reference and predicted output, $\hat{\mathbf{y}}$, for sake of example. The optimization is done through the calculation of an optimum control sequence, $\hat{\mathbf{u}}$, over the control horizon, c ;
- 3) the first element of the control sequence is associated to the control input, $\mathbf{u}(k)$, and sent it to the system;
- 4) this process is repeated until $k = N$.

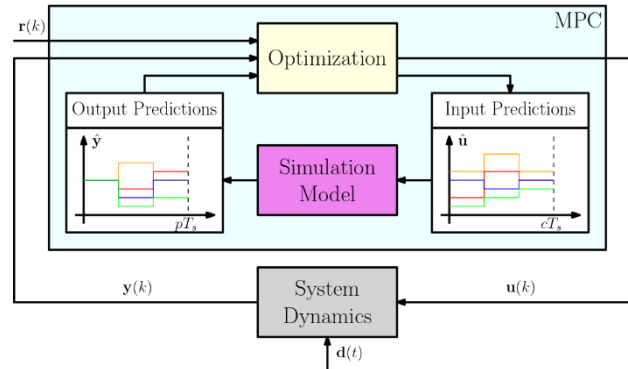


Figure 2. Block diagram of the MPC, adapted from University of Stuttgart [12]

For the MPC design, it is considered a time-varying state-space form of the linearized version of the dynamic model given by the Eq. (1). So, let $\mathbf{x} = [\mathbf{q}, \dot{\mathbf{q}}]^T$ be the state vector. Also, define $\mathbf{u} = \mathbf{f}(t)$ and $\mathbf{w} = [w_1, w_2]^T = [U_{\infty}, \dot{U}_{\infty}]^T$ as the control input and disturbances input vector, respectively. Thus, based on Terry et al. [13], the state-space model of the UDIP can be written as follows:

$$\dot{\mathbf{x}} = \mathbf{A}(\mathbf{x})\mathbf{x} + \mathbf{B}(\mathbf{x})\mathbf{u} + \mathbf{L}(\mathbf{x})\mathbf{w}, \quad (11)$$

where,

$$\mathbf{A}(\mathbf{x}) = \begin{bmatrix} \mathbf{0} & \mathbf{1} \\ -\mathbf{M}(\mathbf{q})^{-1} \frac{\partial \mathbf{G}(\mathbf{q})}{\partial \mathbf{q}} - \mathbf{M}(\mathbf{q})^{-1} \frac{\partial \mathbf{D}(\mathbf{q}, \dot{\mathbf{q}}, w_1)}{\partial \mathbf{q}} & -\mathbf{M}(\mathbf{q})^{-1} \mathbf{C}(\mathbf{q}, \dot{\mathbf{q}}) - \mathbf{M}(\mathbf{q})^{-1} \frac{\partial \mathbf{D}(\mathbf{q}, \dot{\mathbf{q}}, w_1)}{\partial \dot{\mathbf{q}}} \end{bmatrix}; \quad \mathbf{B}(\mathbf{x}) = \mathbf{B}_u(\mathbf{x})\mathbf{o}_u; \quad \mathbf{L}(\mathbf{x}) = \mathbf{L}_w(\mathbf{x})\mathbf{o}_w, \quad (12)$$

$$\mathbf{B}_u(\mathbf{x}) = \begin{bmatrix} \mathbf{0} \\ \mathbf{M}(\mathbf{q})^{-1} \end{bmatrix}; \quad \mathbf{L}_w(\mathbf{x}) = \begin{bmatrix} \mathbf{0} & \mathbf{0} \\ \mathbf{M}(\mathbf{q})^{-1} \mathbf{C}_{\text{FKA}}(\mathbf{q}, \dot{\mathbf{q}}) - \mathbf{M}(\mathbf{q})^{-1} \frac{\partial \mathbf{D}(\mathbf{q}, \dot{\mathbf{q}}, w_1)}{\partial w_1} & \mathbf{M}(\mathbf{q})^{-1} \mathbf{M}_{\text{FKA}}(\mathbf{q}) \end{bmatrix}; \quad \mathbf{o}_u = \begin{bmatrix} 1 \\ 0 \\ 0 \end{bmatrix}; \quad \mathbf{o}_w = \begin{bmatrix} \mathbf{o}_u & \mathbf{0} \\ \mathbf{0} & \mathbf{o}_u \end{bmatrix},$$

with $\mathbf{1}$ and $\mathbf{0}$ as the identity and zero matrices with appropriate dimensions, respectively.

Based on Jagtap et al. [14], the discrete form of the Eq. (11) is given by:

$$\begin{aligned} \mathbf{x}(k+1) &= \mathbf{A}_d(k)\mathbf{x}(k) + \mathbf{B}_d(k)\mathbf{u}(k) + \mathbf{L}_d(k)\mathbf{w}(k) \\ \mathbf{y}(k+1) &= \mathbf{x}(k+1) \end{aligned}, \quad (13)$$

where $\mathbf{x}(k)$, $\mathbf{y}(k)$, $\mathbf{u}(k)$ and $\mathbf{w}(k)$ are the states vector, output vector, control input and disturbances input vector in the discrete form, respectively; $\mathbf{A}_d(k)$, $\mathbf{B}_d(k)$ and $\mathbf{L}_d(k)$ are the discrete version of the state matrices, calculated through the Euler method: $\mathbf{A}_d(k) = (\mathbf{I} + \mathbf{A}(\mathbf{x})T_s)|_{\mathbf{x}=\mathbf{x}(k)}$, $\mathbf{B}_d(k) = (\mathbf{B}(\mathbf{x})T_s)|_{\mathbf{x}=\mathbf{x}(k)}$ and $\mathbf{L}_d(k) = (\mathbf{L}(\mathbf{x})T_s)|_{\mathbf{x}=\mathbf{x}(k)}$.

Following Budiyo [15], the predicted outputs are given by the iteration of the discrete model given by the Eq. (13) in each prediction step, with $i=1,2,\dots,p$ steps, as shown below:

$$\hat{\mathbf{y}}(k+i) = \hat{\mathbf{x}}(k+i) = \mathbf{A}_d^i(k)\mathbf{x}(k) + \sum_{j=1}^i \mathbf{A}_d^{i-j}(k)(\mathbf{B}_d(k)\hat{\mathbf{u}}(k+j) + \mathbf{L}_d(k)\mathbf{w}(k)), \quad (14)$$

Thus, based on the Eq. (14) and considering $\hat{\mathbf{u}}(k+i) = \hat{\mathbf{u}}(k+c-1)$; $c \leq i \leq p-1$, the predicted outputs vectors can be rearranged as follows (the step dependency is not used on the state matrices for sake of notation simplicity):

$$\underbrace{\begin{bmatrix} \hat{\mathbf{y}}(k+1) \\ \hat{\mathbf{y}}(k+2) \\ \vdots \\ \hat{\mathbf{y}}(k+p) \end{bmatrix}}_{\hat{\mathbf{y}}} = \underbrace{\begin{bmatrix} \mathbf{A}_d \\ \mathbf{A}_d^2 \\ \vdots \\ \mathbf{A}_d^p \end{bmatrix}}_{\mathbf{S}_x} \tilde{\mathbf{x}}_0 + \underbrace{\begin{bmatrix} \mathbf{B}_d & 0 & \cdots & 0 \\ \mathbf{A}_d\mathbf{B}_d & \mathbf{B}_d & \cdots & 0 \\ \vdots & \vdots & \ddots & \vdots \\ \mathbf{A}_d^{p-1}\mathbf{B}_d & \mathbf{A}_d^{p-2}\mathbf{B}_d & \cdots & \mathbf{A}_d^{p-c}\mathbf{B}_d \end{bmatrix}}_{\mathbf{S}_u} \underbrace{\begin{bmatrix} \hat{\mathbf{u}}(k) \\ \hat{\mathbf{u}}(k+1) \\ \vdots \\ \hat{\mathbf{u}}(k+c-1) \end{bmatrix}}_{\hat{\mathbf{u}}} + \underbrace{\begin{bmatrix} \mathbf{L}_d & 0 & \cdots & 0 \\ \mathbf{A}_d\mathbf{L}_d & \mathbf{L}_d & \cdots & 0 \\ \vdots & \vdots & \ddots & \vdots \\ \mathbf{A}_d^{p-1}\mathbf{L}_d & \mathbf{A}_d^{p-2}\mathbf{L}_d & \cdots & \mathbf{L}_d \end{bmatrix}}_{\mathbf{S}_d} \tilde{\mathbf{w}}_0, \quad (15)$$

being $\tilde{\mathbf{x}}_0 = [\mathbf{x}(k), \dots, \mathbf{x}(k)]^T$ and $\tilde{\mathbf{w}}_0 = [\mathbf{w}(k), \dots, \mathbf{w}(k)]^T$ the augmented states and disturbances vectors at the k -th step.

As in Jagtap et al. [14], the objective of the MPC is to minimize the quadratic cost function of Eq. (16, on the left side). After some algebraic manipulation, the optimization can be rewritten as a quadratic programming (QP) problem, as shown on the Eq. (16, on the right side):

$$\begin{aligned} \min_{\hat{\mathbf{u}}(c)} J(\mathbf{x}_0, \hat{\mathbf{u}}) &= (\hat{\mathbf{y}} - \tilde{\mathbf{r}})^T \tilde{\mathbf{Q}}(\hat{\mathbf{y}} - \tilde{\mathbf{r}}) + \hat{\mathbf{u}}^T \tilde{\mathbf{R}}\hat{\mathbf{u}} & \min_{\hat{\mathbf{u}}(c)} J(\mathbf{x}_0, \hat{\mathbf{u}}) &= \hat{\mathbf{u}}^T \mathbf{H}\hat{\mathbf{u}} + \mathbf{F}\hat{\mathbf{u}} \\ \text{subject to: } \hat{\mathbf{y}} &= \mathbf{S}_x \mathbf{x}_0 + \mathbf{S}_u \hat{\mathbf{u}} + \mathbf{S}_d \mathbf{w}_0 & \Leftrightarrow \text{subject to: } \mathbf{G}\hat{\mathbf{u}} &\geq \mathbf{h} \\ & \tilde{\mathbf{u}}_{\min} \leq \hat{\mathbf{u}} \leq \tilde{\mathbf{u}}_{\max} \end{aligned} \quad (16)$$

with $\tilde{\mathbf{r}} = [\mathbf{r}(k+1), \mathbf{r}(k+2), \dots, \mathbf{r}(k+p)]^T$, $\tilde{\mathbf{Q}} = \text{blockdiag}(\mathbf{Q}, \mathbf{Q}, \dots, \mathbf{P})$ and $\tilde{\mathbf{R}} = \text{diag}(\mathbf{R}, \mathbf{R}, \dots, \mathbf{R})$, where $\mathbf{r}(k+i)$ is the reference at the i -th prediction time step, \mathbf{Q} and \mathbf{R} are weighting matrices for the tracking errors and control efforts, respectively, while \mathbf{P} is the terminal weighting matrix used to enforce the closed-loop stability; the terms of the QP problem follows: $\mathbf{H} = \mathbf{S}_d^T \tilde{\mathbf{Q}} \mathbf{S}_d + \tilde{\mathbf{R}}$, $\mathbf{F} = 2(\mathbf{S}_x^T \tilde{\mathbf{x}}_0^T + \mathbf{S}_d^T \tilde{\mathbf{w}}_0^T - \tilde{\mathbf{r}}^T) \tilde{\mathbf{Q}} \mathbf{S}_u$, $\mathbf{G} = \text{diag}(-\mathbf{I}, +\mathbf{I})$ and $\mathbf{h} = [-\tilde{\mathbf{u}}_{\min}, +\tilde{\mathbf{u}}_{\max}]^T$.

4 Results

Numerical simulations were conducted to verify the effectiveness of the proposed controller. The simulation scenario is based on the set-point regulation/stabilization problem. In this case, the objective of the controller is to make the system reaches and maintaining a set-point for the cart while stabilize the double pendulum on the vertical position, referring to the unstable equilibrium point. The simulations were performed considering two scenarios: 1) in the absence of disturbances, and 2) in the presence of a time-varying water current. The simulations were done in the MATLAB/Simulink® environment, considering the 5-th order Dormand-Prince method with a fixed time step of 0.001 (s) for the numerical integration of the nonlinear model in state-space form. The controller is implemented with the MPC Toolbox™ of MATLAB® considering a rate frequency of 10 (Hz). Table 1 shown the simulations parameters.

Table 1. Simulation parameters

Symbols (Π_i ; $i=1,2,3$ and $\Pi_2 = \Pi_3$)	Values	Units (SI)
$\{\mathbf{B}_1, \mathbf{H}_1, \mathbf{L}_1, \mathbf{I}_{O_1 O_1+1}, \mathbf{I}_{O_1 CG_1}, \mathbf{I}_{O_1 CB_1}, D_1, \Delta_1\}$, dims.	{0.15, 0.15, 0.20, 0.50, 0.25, 0.25, 0.05, 0.10}	(m)
$\{C_{D_{xx1}}, C_{D_{yy1}}\}$, drag coefficients	{2.0, 0, 0.60, 2.0}	(-)
$\mathbf{M}_{RB,i}$, rigid body mass matrix	diag{12.15, 12.15, 0}; diag{2.65, 2.65, 0.06}	(kg; kg; kgm ²)
$\hat{\mathbf{M}}_{FKA,i} \cong \hat{\mathbf{M}}_{A,i}$, added mass tensor	diag{4.50, 4.50, 0}; diag{0.27, 0.98, 0.02}	(kg; kg; kgm ²)
p, c ; \mathbf{Q} ; \mathbf{P} ; \mathbf{R} , MPC's parameters	20, 5; diag{60, 20, 20, 0, 0, 0}; diag{90, 40, 40, 0, 0, 0}; 0.1	(-)

The parameters were calculated considering aluminum as the bodies' material and the formulation presented in Newman [10] and Fossen [11] for the local tensors. The drag coefficients were extracted from Leabourne and Rock [8]. Other parameters of the simulations are: $g = 9.81$ (m/s²), $\rho = 1000$ (kg/m³), $C_{D,cc} = 0.80$ (-), $T_s = 0.1$ (s) and $\mathbf{u}_{\max} = -\mathbf{u}_{\min} = 60$ (N). Also, the water current considered in the scenario (2) is given by: $U_\infty(t) = A_\infty \sin(\omega_\infty t) + \delta_\infty$, where $A_\infty = 0.1$ (m/s), $\omega_\infty = 0.63$ (rad/s) and $\delta_\infty = 0.05$ (m/s).

To verify the stabilization proprieties of the MPC at the initials instants, a misalignment between the pendulum's links and the vertical direction is introduced in the initial conditions, as follows: $\theta_1(0) = \theta_2(0) = 0.2$ (rad). The other initial states for the numerical simulation a set to zero, thus: $\mathbf{x}(0) = [0, 0.2, 0.2, 0, 0]^T$ (SI).

The simulations' results of the scenarios (1) and (2) are shown in Figure 3 (i)-(iv) and (v)-(viii), respectively.

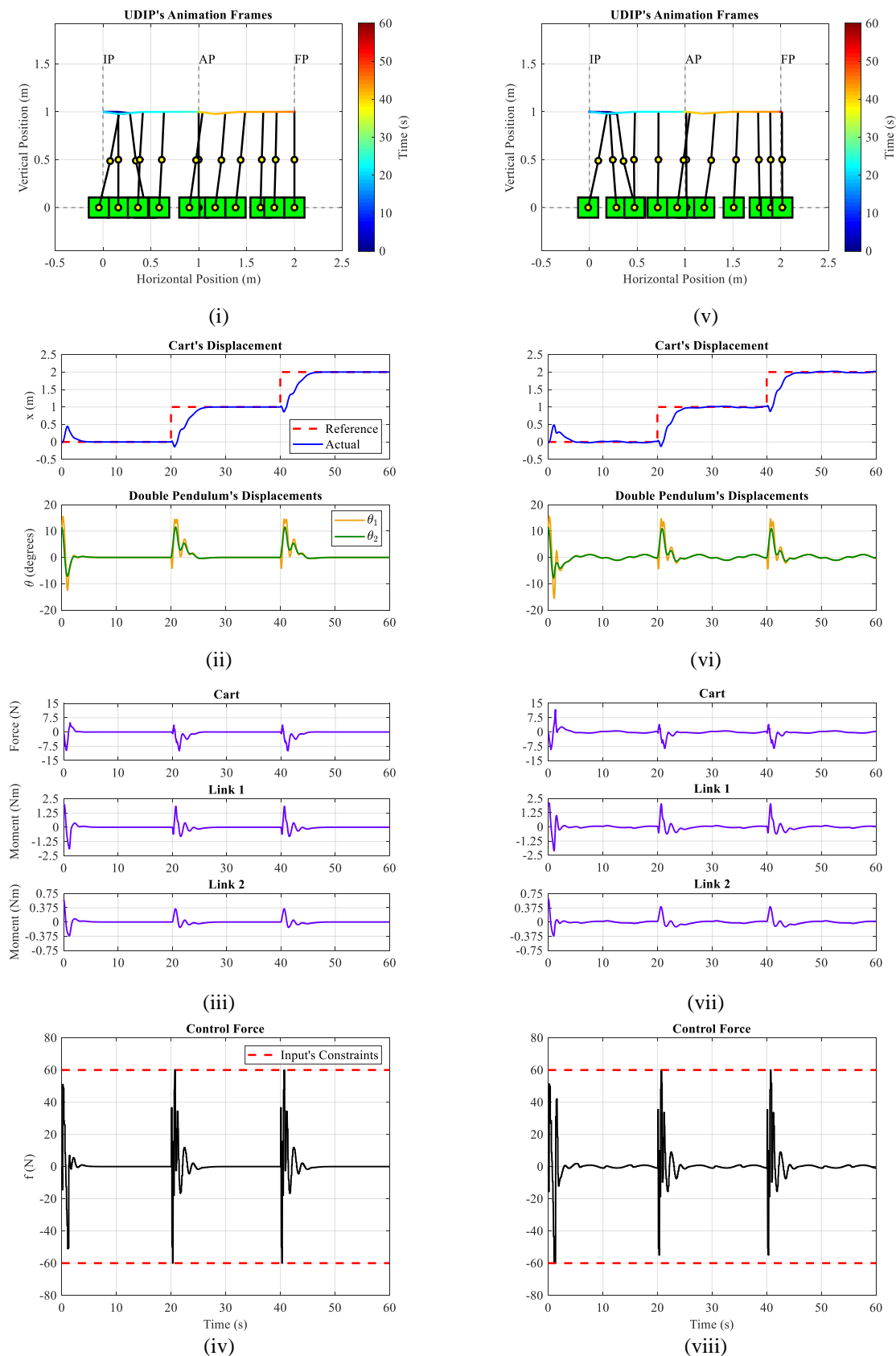


Figure 3. UDIP's frames (i)-(ii); States history (iii)-(iv); Hydrodynamic forces (v)-(vi); Control forces (vii)-(viii); Scenario (1) – without disturbance – (i)-(iv); Scenario (2) – with disturbances (water current) – (v)-(viii)

Figure 3 (i; v) shown the traced path of the end-effector (with a color gradient denoting the simulation step time) together with a sample of the animation frames. Figure 3 (i; v) also shown the reference positions denoted as Initial Position (IP), Average Position (AP), and Final Position (FP), which are represented by vertical dashed lines. The time history of the generalized coordinates is shown in Figure 3 (ii; vi), where it can be seen that in both simulation cases the MPC meets the performance requirements for the set-point regulation of the cart's displacement while performs the stabilization of the pendulum's joints. However, in Figure 3 (vi) of the scenario (2), it is noted a slow oscillation on the steady-state of those displacements. This behavior can also be observed on the end-effector path in Figure 3 (v), where the AP and FP are not exactly reached in comparison with Figure 3 (i) of the scenario (1). This is due to a qualitative change of the dynamics that is induced by the water current, as can be seen on time history of the generalized hydrodynamic forces in Figure 3 (iii; vii), where a slow oscillation is also verified in Figure 3 (vii) of the scenario (2). Thus, the underwater current has a considerable impact on the system's dynamics. Nonetheless, the proposed MPC is formulated based on a well-structured dynamic model, in the sense of the correct incorporation of the water current effects on its predictions, therefore, this can handle well such kind of disturbances (assuming that those can be measured) with a minimum impact on the set-point regulation problem in comparison with the scenario (1). Regarding the control input shown in Figure 3 (iv; viii), it is seen that the MPC meets the saturation limits imposed during the optimization process, working inside the allowed region in all the simulation for both scenarios. This observation is also a requirement for the control system since these limits must be defined according to the actuator. Moreover, comparing Figure 3 (iv) and (viii), it is observed a slow oscillation in the control force for the scenario (2) on the platoons referring to the steady-state. According to the previous observations, this is related to the disturbances induced by the water current, which produces an increase in the control effort, defined here as: $E = \sum_{k=1}^N |u_k|$. For the scenario (1), a $E = 162.5$ was obtained, whereas for the scenario (2), with disturbances, a $E = 203.8$ was found. Then, the disturbances induced by the water current results in a significative increase in the control effort ($\sim 25.4\%$), as already expected. In fact, such an observation can reflect some of the control problems of autonomous underwater robotics systems in unstructured environments, subjected to disturbances. In these systems, the amount of power available is defined by its batteries, therefore, any unsuspected increase in the control effort can harm its autonomy.

5 Conclusions

In this paper, it is presented a detailed modeling of an UDIP using the formalism of the Analytical Mechanics and considering the most relevant hydrodynamic and hydrostatic effects. Due to its completeness, the developed model can be used as a new benchmark model for control system design considering underwater robotics aspects for general multibody systems. Based on the developed model, it is proposed an adaptive discrete-time MPC considering the disturbances induced by a time-varying water current. The proposed controller is tested by means of numerical simulations in different scenarios to verify its performance. In those tests, the controller performed well for both scenarios. However, many improvements can be made. The MPC can be extended to include other disturbances effects, such as wave-induced forces, if a suitable mathematical model is available. In this sense, an observer scheme for the disturbances can be added to the controller. Such a scheme can be made inside the predictive model or outside, with an ad-hoc observer based on the Kalman filter algorithm. Also, it is known that the actuators have a considerable impact on the system's dynamics, while the sensors' feedback can be very degrading to the control performance. Due to these reasons, it must be considered in the presented formulation. As well, the robustness of the proposed controller to model's parameters variation needs to be verified, since the parameters of the hydrodynamics forces can change significantly according to the flow conditions. Finally, the authors believe that, through necessary modifications, the proposed MPC can be applied to more complex underwater multibody systems (e.g., UVMSs).

References

- [1] Moss, W.F., "Vertical stabilization of a rocket on a movable platform", *Applied Mathematical Modeling. A multidisciplinary approach: A multidisciplinary approach*, pp. 363-381., 1997.
- [2] Rusaw, D.F., Ramstrand, S., "Validation of the Inverted Pendulum Model in standing for transtibial prosthesis users", *Clinical Biomechanics*, vol. 31, pp. 100-106, 2016.
- [3] Sultan, G.A. and Farej, Z.K.A., "Design and Performance Analysis of LQR Controller for Stabilizing Double Inverted Pendulum System", *Circulation in Computer Science Vol.2, No.9, Mosul, Iraq*, pp. 1-5, 2017.
- [4] Moysis, L., "Balancing a double inverted pendulum using optimal control and Laguerre functions", technical report, Aristotle University of Thessaloniki, Greece, 2016.

- [5] Krafes, S., Chalh, Z., Saka, A., “Review: Linear, nonlinear and intelligent controllers for the inverted pendulum problem”, 2nd International Conference on Electrical and Information Technologies ICEIT’2016, Sidi Mohammed Ben Abdellah University Fez, Morocco, 2016.
- [6] Mohan, V., Rani, A., Singh V., “Robust adaptive fuzzy controller applied to double inverted pendulum”, Journal of Intelligent & Fuzzy Systems, ICE Division, Netaji Subhas Institute of Technology, New Delhi, India, 2017.
- [7] Hasnain, S., Hameed, S.U., Choi, S.-H., Hong, K.-S., “Dynamics and Vibrational Control of an Underwater Inverted Pendulum”, 16th International Conference on Control, Automation and Systems (ICCAS 2016), School of Mechanical Engineering, Pusan National University, Busan, Republic of Korea, 2016.
- [8] Leabourne, K.N., Rock, S.M., “Model Development Of An Underwater Manipulator For Coordinated Arm-Vehicle Control”, The International Journal of Robotics Research, vol. 2, pp. 941-946, 1998.
- [9] McLain, T.W., Rock, S.M., “Development and Experimental Validation of an Underwater Manipulator Hydrodynamic Model”, The International Journal of Robotics Research, vol. 17, n. 7, pp. 748-759, 1998.
- [10] Newman, J.M., “Marine Hydrodynamics”, Mit Press, 1977.
- [11] Fossen, T.I., “Guidance and Control of Ocean Vehicles”, Wiley-Blackwell, 1998.
- [12] University of Stuttgart, “Model predictive control”, Institute for Systems Theory and Automatic Control, Available in: <https://www.ist.uni-stuttgart.de/research/topics/mpc/>, Accessed: March 26th, 2020.
- [13] Terry, J., Rupert, L., Killpack, M., “Comparison of linearized dynamic robot manipulator models for model predictive control”, 2017 IEEE-RAS 17th International Conference on Humanoid Robotics (Humanoids), pp. 205-212, 2017.
- [14] Jagtap, P., Raut, P., Kumar, P., Gupta, A., Singh, N.M., Kazi, F., “Control of Autonomous Underwater Vehicle using Reduced Order Model Predictive Control in Three Dimensional Space”, IFAC-PapersOnLine, vol. 49, pp. 772-777, 2016.
- [15] Budiyo, A., “Model predictive control for autonomous underwater vehicles”, Indian Journal of Geo-Marine Sciences, vol. 40, pp. 191-199, 2011.

Acknowledgements. The first and fourth authors acknowledge CAPES for Ph.D. scholarships. The PUB/PAPFE of USP is also acknowledged for the undergraduate scholarship of the third author.

Authorship statement. The authors hereby confirm that they are the sole liable persons responsible for the authorship of this work, and that all material that has been herein included as part of the present paper is either the property (and authorship) of the authors, or has the permission of the owners to be included here.